NESTED-MEMS TEMPERATURE COMPENSATED SINGLE-CRYSTALLINE SILICON OSCILLATOR

Amir Rahafrooz, Diego Emilio Serrano, Ryan Hennessy, William McDonald, Duane Younkin, Kieran Nunan, Stanley Che, and Ijaz Jafri*
Panasonic Massachusetts Laboratory, Waltham, Massachusetts, USA

ABSTRACT

This paper introduces an innovative dual-mode temperature-compensated silicon MEMS oscillator, featuring a distinctive architecture comprised of two compact bulk acoustic wave (BAW) resonators operating in their Breathing and Lamé resonance modes. The Breathing mode, characterized by a low temperature coefficient of frequency (TCF), functions as the reference clock, while the Lamé mode, with a significantly higher TCF, serves as a temperature sensor. A Nested-MEMS design incorporates a circuit that generates a clock based on the low TCF reference oscillator, feeding it into a closed-loop temperature-to-digital converter (TDC). The TDC employs the high-TCF Lamé-mode resonator to ensure that it consistently operates at its resonance frequency. Consequently, the control signal produced by the proportional-integral-derivative (PID) controller is directly related to the frequency ratio and is used for temperature compensation. The proposed architecture is implemented using an FPGA-based system, demonstrating impressive performance with output frequency variation limited to ±125 parts per billion (ppb) across a temperature range of 10°C to 70°C. The integration of this dual-mode oscillator streamlines the design by requiring only one drive loop, thereby reducing power consumption.

KEYWORDS

Temperature Compensated MEMS Oscillator, Dual-Mode MEMS Oscillator, Nested-MEMS Dual-mode Temperature to Digital Converter

INTRODUCTION

Oscillators are fundamental components in a myriad of electronic systems, serving as critical timing references for various applications across industries. Their applications span from communication systems to consumer electronics. Moreover, they play pivotal roles in navigation systems, medical devices, and precision instrumentation, among others. Traditionally, quartz oscillators have been the cornerstone of timing solutions. However, recent years have witnessed the emergence of Microelectromechanical Systems (MEMS) oscillators as viable alternatives. These devices have gradually penetrated the market and captured a significant share thereof. This transition has been driven by the inherent advantages of MEMS resonators, including their compactness, robustness against shock, low-cost batch fabrication, and enhanced reliability compared to conventional quartz counterparts [1].

Despite their advantages, MEMS resonators have faced the notable challenge of having a large sensitivity of resonance frequency to temperature. To address this issue, various methods for temperature compensation of MEMS resonators have been developed. These methods encompass both passive and active techniques aimed at mitigating the impact of temperature fluctuations on resonance frequency.

Passive temperature compensation techniques focus on modifying the resonator's design or composition to inherently counteract or change the effects of temperature. For instance, designs incorporating thermal stress profiles across temperature [2] or composite materials with opposite TCF [3, 4] have shown promise in reducing temperature sensitivity. Additionally, degenerative doping of semiconductor materials [5, 6] has been utilized to modify the Young's modulus dependencies across temperature, effectively reducing TCF components without compromising performance. While composite material can impact thermoelastic damping, degenerate doping has no impact, providing a better option to achieve high quality factors and lower noise in monolithic resonators.

Even with passive compensation techniques, residual temperature variations may still exist, necessitating the adoption of active temperature compensation methods. These techniques dynamically adjust the output frequency in response to temperature changes to maintain stable operation. Electronic tuning is one of the active techniques widely used in products. Electronic tuning utilizes a temperature sensor and a temperature to digital converter (TDC) to create a change that is opposite to change in TCF of the reference resonator. It then uses a frequency synthesizer to adjust the frequency of the reference resonator using TCD output. One possible implementation is to utilize a thermistor next to the MEMS resonator [7]; however, this approach may not satisfy the stringent hysteresis, aging, and temperature performance required for some applications. Dual-mode approaches [8-12] involve using two resonance modes belonging to one or two adjacent resonance bodies. The modes are designed to have different TCFs and are brought into vibration using two separate oscillation loops. The temperature is then deduced from the change in frequency of one or a combination of both of modes. This method improves hysteresis and provides lower variation across temperature at the cost of adding an additional drive loop and the power consumption associated with it. In this context, dual-mode temperature-compensated MEMS oscillators have emerged as a promising solution. By leveraging two resonance modes with different TCFs, these oscillators can achieve improved temperature stability.

In this paper, we present a novel dual-mode temperature-compensated MEMS oscillator that utilizes a single oscillation drive loop. We begin by discussing the design and characterization of the MEMS resonator pair implemented in a highly doped silicon substrate. Subsequently, we unveil the Nested-MEMS architecture [13], which forms the basis for our oscillator implementation. Following this, we showcase the interfacing of MEMS resonators with an FPGA-based implementation of the Nested-MEMS architecture, substantiating the efficacy of our methodology. Finally, we present characterization results of the oscillator, highlighting its remarkable temperature stability and performance. We conclude by summarizing our findings and outlining future avenues for exploration.

MEMS RESONATORS

The dual-mode oscillator employes two high frequency MEMS resonators. The reference resonator, utilized for generating the primary clock signal, should possess a relatively low TCF to ensure stable operation across temperature. Conversely, the temperature-sensor resonator requires a pronounced TCF to enhance its sensitivity for temperature sensing. Additionally, minimizing the footprint of both resonators and positioning them in close proximity ensures that they both experience the same temperature.

978-1-940470-05-4/HH2024/$25©2024TRF
DOI 10.31438/TRF.HH2024.9

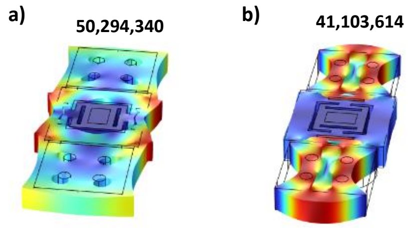

Figure 1: Mode shapes and resonance frequencies for a) Breathing mode resonator and b) Lamé mode resonator. The resonators are along <100> crystalline orientation. Color coding denotes total displacement, with red indicating maximum displacement and blue representing minimum displacement.

Resonator Design

In the presented design, a single MEMS die contains two resonators (Fig 2a). Each resonator is comprised of two in-phase vibrating proof masses connected via a decoupling structure connected to a central anchor. This decoupling structure is specifically tailored to minimize support loss across fabrication process variations. Additionally, a central anchor minimizes susceptibility to die stress, boundary condition changes, and hysteresis effects. One resonator is optimized for operation in a breathing mode of vibration at 50.3 MHz, while the other is tailored for a Lamé mode of vibration at 41.1 MHz. Fig 1 illustrates the resonant mode shapes for both resonators. These resonators are oriented along the <100> crystalline orientation, ensuring a low TCF for the breathing mode. The Lamé resonator, with its inherently higher TCF, is designated for temperature sensing.

Perfectly matched layers simulation was run to minimize support loss on both resonators resulting in Q_{Support} values exceeding 200 M and 2 B across process variations for Breathing and Lamé resonators respectively. Thermoelastic damping simulation yielded Q_{TED} values of 1.24 M and 425 k for the respective resonators.

Fabrication

The two resonators were instanced next to each other to form a single MEMS die. Electrodes were placed around each resonator to operate them through electrostatic transduction. The resonators were fabricated on SOI wafers with 20 µm device layer and 2 µm of buffer oxide layer thickness. The device layer is Phosphorus-doped single crystalline silicon with resistivity of 0.0016 to 0.0018 Ω.cm that translates to dopant concertation of 4.07e19 to 4.65e19 cm^{-3}. The devices were fabricated using the HARPSS [15] process with transduction gap of 200 nm, then bonded to cap wafer resulting in package pressure of < 0.1 Torr. The resonators are electrically connected to the handle layer through polysilicon plugs which are used to apply a polarization voltage to the resonator body. Through

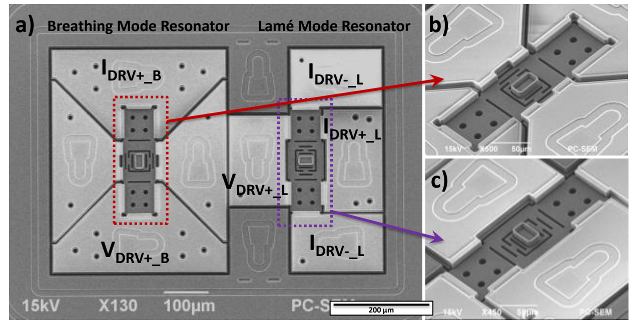

Figure 2: a) Top SEM view of the MEMS die comprised of two resonators for dual-mode operation along with electrode configuration. Areas with brighter colors are electrostatic electrodes around the resonators. The holes on electrodes are to release parts of buffer oxide layer underneath electrodes, reducing capacitance to handle layer. b) SEM view of Breathing mode resonator c) SEM view of Lamé mode resonator.

silicon vias (TSVs) in the cap wafer carry signals from the MEMS electrodes to the metalized pads on top of the packaged device. Fig 2 shows the SEM view of the two resonators and the utilized electrode configuration before bonding to the cap wafer.

Characterization

Full wafers of capped resonators were characterized for frequency and quality factor. Figures 3.a and 3.b depict the color maps of measured resonance frequencies across a wafer for the Breathing and Lamé resonators, respectively. Additionally, Figure 3.c illustrates the distributions of measured quality factors for both modes, indicating 105,000 for Breathing and 135,000 for Lamé resonators. Table 1 presents both modeled and measured Q factors.

Table 1: Modeled and measured quality factor values. Maximum expected Q values are calculated based on modeled $Q_{support}$, Q_{TED} and expected f.Q limit for single crystalline silicon (2×10^{13}) [16]

Resonator	Freq. (MHz)	Modeled $Q_{Support}$	Modeled Q_{TED}	Max. Expected Q	Measured Q	Measured $f.Q$
Breathing	50.3	200 M	1.24 M	302 k	105 k	5.2×10^{12}
Lamé	41.1	2 B	425 k	227 k	135 k	5.5×10^{12}

Following the dicing of wafers, singulated MEMS dies underwent characterization using an oven to observe the impact of temperature on resonance frequency and quality factor. Figure 3.d shows the quality factors for both modes against temperature. Notably, while the quality factor of Lamé resonators decreases at higher temperatures, the quality factor of the Breathing mode remains relatively constant. This constant quality factor for the Breathing resonator suggests a design dominated by support loss.

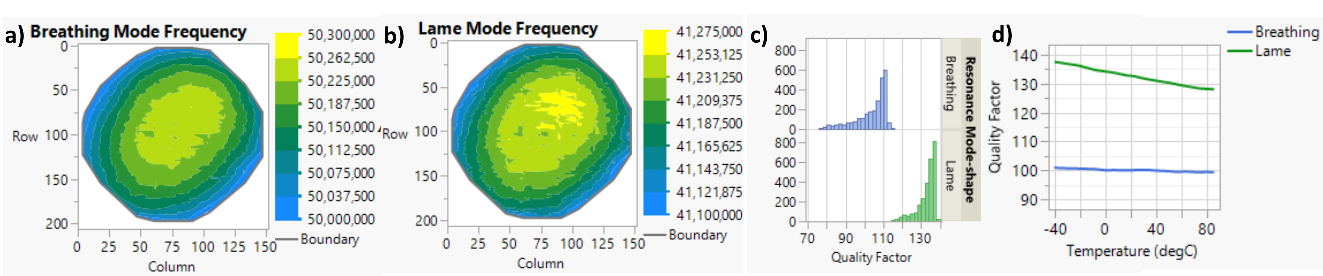

Figure 3: Measured resonant frequency across wafer for a) Breathing mode resonator, b) Lamé mode resonator, c) measured quality factor distribution for both resonators, d) measured quality factors across temperature.

Furthermore, resonance frequencies were recorded across temperature. Fig 4 shows the frequency variations for both resonance modes and their frequency ratio, which closely align with the simulations conducted using the material properties from [14].

In Table 1 measured quality factors fall notably below the anticipated Q limit for each resonator obtained based on modeled $Q_{Support}$, Q_{TED} and known $f.Q$ limit for Single crystalline silicon [16]. This suggests that actual support loss may exceed the expected values, thereby impacting overall quality factor. One potential explanation is the sensitivity of support loss to specific fabrication imperfections not accounted for in the FEA model. Even after extensive modeling and incorporating a wide range of imperfections, the results from perfectly matched layers did not align well with measured Q factors.

Another possible cause could be inaccurate material properties used for simulation. This discrepancy can manifest in two ways: firstly, it may alter the resonance frequencies of target modes relative to nearby spurious modes, causing them to interact and affect Q. Secondly, slight variations in mode shape and frequency might increase sensitivity to fabrication imperfections. A closer examination of the Breathing mode, which exhibited a larger Q discrepancy, reveals that the decoupling structure experienced significant displacement, rendering it more susceptible to imperfections. Designing a new structure with lower displacement in the decoupling mechanism could mitigate this sensitivity to process variations.

NESTED-MEMS ARCHITECTURE

Nested-MEMS represents a dual-mode architecture where the low-TCF breathing-mode resonator serves as the reference clock for a closed-loop temperature-to-digital converter (TDC), leveraging the high-TCF Lamé-mode resonator as a temperature reference (Fig 5). The TDC incorporates a PID controller to finely adjust a fractional-N PLL, ensuring precise resonance frequency excitation of the temperature-reference resonator. Consequently, the PID-generated control signal correlates with the frequency ratio of the

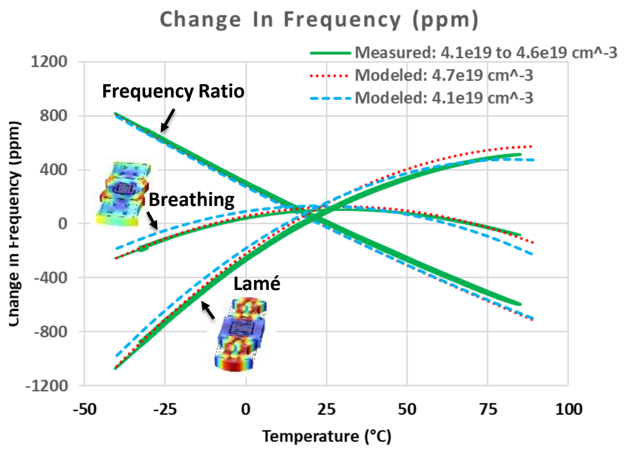

Figure 4: Variations in frequency in ppm for Breathing mode resonator, Lamé mode resonator and the frequency ratio (Breathing/Lamé). Measurements in green are in very good agreement obtained from FEA simulation shown in red and blue. Doping level concentrations for the three curves are specified in the legend. SOI manufacture has specified a range where upper and lower limits are very close to the doping levels for the two material properties used for FEA simulation.

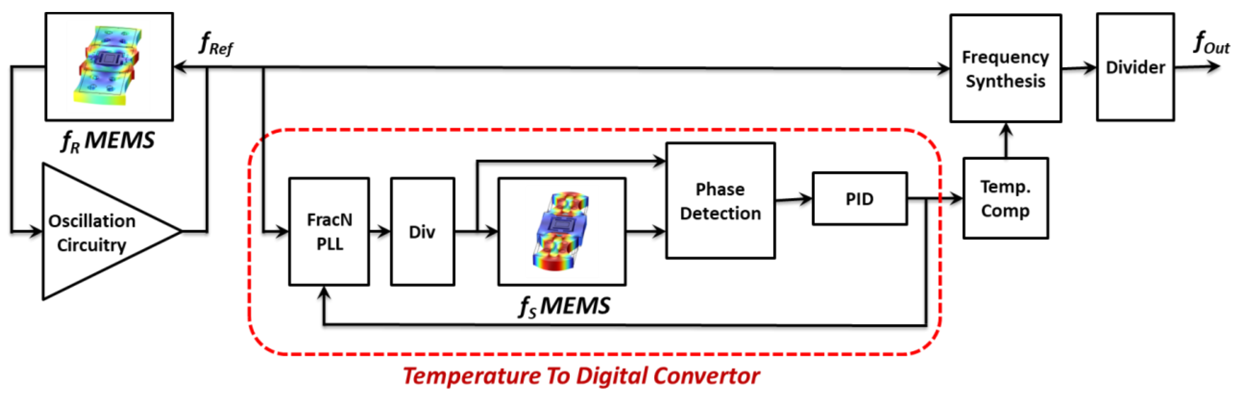

Figure 5: Block diagram of Nested-MEMS architecture

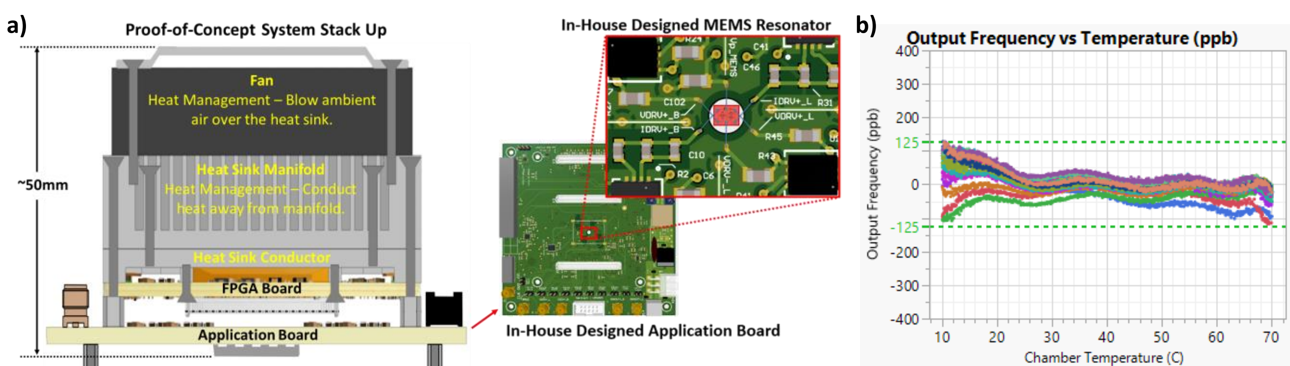

Figure 6: a) Picture of the FPGA board as well an application board to interface with the MEMS die used to implement Nested-MEMS Architecture b) Measured variations in output frequency during 16 ramps up and down cycles across temperature.

temperature and reference oscillators, enabling effective compensation of the reference clock with minimal aging effects. One of the main strengths of this architecture compared to other dual-mode systems is that, instead of utilizing two oscillation loops, it uses only one for the reference clock, resulting in lower power.

The proof-of-concept Nested-MEMS architecture was implemented using the FPGA-based system shown in Fig 6.a. The system is composed of an FPGA KRM-4ZU47DR module that is mounted onto an application board. The board houses the MEMS die, the transimpedance amplifiers, and drivers acting as the analog interface between the two resonators and the FPGA board.

In an ideal scenario, the temperature compensation block should be able to apply the inverse of the normalized reference mode variations to the frequency synthesis block across temperature. To calibrate the temperature compensation block, the system was placed inside an oven and both modes were operated in a close-loop configuration to record the resonance frequencies across temperature. The reference oscillator frequency as a function of the frequency ratio was then fitted with a polynomial, and its coefficients were extracted from the measured data. These values were then programmed into the temperature compensation block.

SYSTEM RESULTS

After performing the calibration, the system was run in the Nested-MEMS configuration while ramping the temperature up and down 16 times from 10 °C to 70 °C with a ramp of 1 °C/minute. The temperature was limited by the range tolerated by FPGA board, which had to be placed inside the oven. The target compensated output frequency was set to 10 MHz. Figure 6.b shows the output frequency variation that falls within ±125 ppb. This variation is in part due to signal to noise ratio and the Nested-MEMS implementation in the FPGA.

CONCLUSION

This article presented a novel dual-mode silicon temperature-compensated oscillator capable of power savings through a single drive-loop, demonstrating ±125 ppb output frequency variation across a temperature range with minimal hysteresis. The two resonator designs utilized for dual-mode operation exhibited TCF values that matched exactly the expectations based on finite element analysis (FEA) simulations.

As a next step, fine-tuning of material properties based on measured TCFs and resonance frequencies for different modes of operation is necessary, serving as feedback for design optimization. Additionally, adjustments in doping levels may be required for optimal operation.

While the FPGA-based implementation of Nested-MEMS successfully validated the architecture, it has limitations including high signal-to-noise ratio (SNR), low speed, limited temperature range, and FPGA capability. Therefore, the next phase involves designing a new application-specific integrated circuit (ASIC) and implementing proper packaging to fully leverage its capabilities in reducing power consumption and improving phase noise.

REFERENCES

[1] G. Wu, J. Xu, E. J. Ng and W. Chen, "MEMS Resonators for Frequency Reference and Timing Applications," in Journal of Microelectromechanical Systems, vol. 29, no. 5, pp. 1137-1166, Oct. 2020.

[2] Wan-Thai Hsu, J. R. Clark and C. T. . -C. Nguyen, "Mechanically temperature-compensated flexural-mode micromechanical resonators," International Electron Devices Meeting 2000. Technical Digest. IEDM (Cat. No.00CH37138), San Francisco, CA, USA, 2000, pp. 399-402.

[3] R. Abdolvand, H. Lavasani, and F. Ayazi, "Thin-film piezoelectric-onsilicon resonators for high-frequency reference oscillator," IEEE Trans. Ultrasonics, Ferroelectrics and Freq. Control, vol. 55, no. 12, pp. 2596-2606, Dec. 2008.

[4] R. Tabrizian, G. Casinovi, and F. Ayazi, "Temperature-stable high-Q AlN-on-silicon resonators with embedded array of oxide pillars," in Proc. Hilton Head Solid-State Sens., Actuators, Microsyst. Workshop, Jun. 2010, pp. 100–101.

[5] A. K. Samarao and F. Ayazi, "Temperature compensation of silicon micromechanical resonators via degenerate doping," in IEDM Tech. Dig., Dec. 2009, pp. 1–4.

[6] A. Hajjam, A. Logan and S. Pourkamali, "Doping-Induced Temperature Compensation of Thermally Actuated High-Frequency Silicon Micromechanical Resonators," in Journal of Microelectromechanical Systems, vol. 21, no. 3, pp. 681-687, June 2012.

[7] R. Melamud, et al., "MEMS Enables Oscillators With Sub-Ppm Frequency Stability And Sub-Ps Jitter," Solid-State Sensors, Actuators, and Microsystems Workshop Hilton Head Island, June 3-7, 2012.

[8] S. Schodowski, "Resonator self-temperature-sensing using a dual-harmonic-mode crystal oscillator," Proceedings of the 43rd Annual Symposium on Frequency Control, Denver, CO, USA, 1989, pp. 2-7.

[9] M. Koskenvuori, V. Kaajakari, T. Mattila and I. Tittonen, "Temperature measurement and compensation based on two vibrating modes of a bulk acoustic mode microresonator," 2008 IEEE 21st International Conference on Micro Electro Mechanical Systems, Tucson, AZ, USA, 2008, pp. 78-81.

[10] J. C. Salvia, R. Melamud, S. A. Chandorkar, S. F. Lord and T. W. Kenny, "Real-Time Temperature Compensation of MEMS Oscillators Using an Integrated Micro-Oven and a Phase-Locked Loop," in Journal of Microelectromechanical Systems, vol. 19, no. 1, pp. 192-201, Feb. 2010.

[11] M. -H. Li, C. -Y. Chen, C. -S. Li, C. -H. Chin and S. -S. Li, "Design and Characterization of a Dual-Mode CMOS-MEMS Resonator for TCF Manipulation," in Journal of Microelectromechanical Systems, vol. 24, no. 2, pp. 446-457, April 2015.

[12] M. Heidarpour Roshan et al., "A MEMS-Assisted Temperature Sensor With 20- μK Resolution, Conversion Rate of 200 S/s, and FOM of 0.04 pJK2," in IEEE Journal of Solid-State Circuits, vol. 52, no. 1, pp. 185-197, Jan. 2017.

[13] D. Younkin, R. J. Lipka, R. Hennessy, D. E. Serrano, C. Che, A. Rahafrooz, M. Maymandinejad, "Real time frequency shift detection via a nested MEMS architecture", Patent Application: US18/149275, Panasonic Corporation, Filed on 1/13/2023.

[14] E. J. Ng, V. A. Hong, Y. Yang, C. H. Ahn, C. L. M. Everhart and T. W. Kenny, "Temperature Dependence of the Elastic Constants of Doped Silicon," in Journal of Microelectromechanical Systems, vol. 24, no. 3, pp. 730-741, June 20.

[15] F. Ayazi, and K. Najafi, "High aspect-ratio combined poly and single-crystal silicon (HARPSS) MEMS technology," Journal of Microelectromechanical Systems, 9(3), 2000, pp.288-294.

[16] Rodriguez, J., Chandorkar, S.A., Watson, C.A. et al. " Direct Detection of Akhiezer Damping in a Silicon MEMS Resonator", Sci Rep 9, 2244, 2019.

CONTACT

*amir.rahafrooz@us.panasonic.com